

A No-Load RF Calorimeter

R. C. Chernoff

R. F. Systems Development Section

A novel RF calorimeter is described and analyzed. The device combines the conservation of energy principle with the dc substitution idea to eliminate the need for RF and/or dc loads, thereby providing highly accurate "on-line" measurements of RF power at low cost. Breadboard test data are reported.

I. General Description

Consider any source, S, of power that accepts dc (or low-frequency) power, P_{dc} , produces output power, P_o , and rejects dissipated power, P_{diss} , to an external heat sink. If P_{dc} , P_o , and P_{diss} are considered average values, conservation of energy implies

$$P_o = P_{dc} - P_{diss} \quad (1)$$

which in turn suggests the analog circuit of Fig. 1 for measuring P_o .

Calibration of the device consists of correct adjustment of both the full scale deflection and zero of the P_o meter. First, with the P_{diss} input to the analog subtractor disconnected, a known value of P_{dc} is applied to the source. The P_o meter is then adjusted by means of potentiometer (pot) R1 to read " P_{dc} ," i.e., that voltage (preferably at or near full-scale) corresponding to P_{dc} . Secondly, the P_o

meter zero is set by pot R2 under the following conditions: (1) P_{diss} inputs is reconnected, (2) some value of $P_{dc} > 0$ is applied to the source, (3) the source is adjusted for zero output.

Since the conservation of energy principle applies to every form of energy, P_o can be any kind of power whatever; the utility of the device depends only on whether P_{dc} is easier to measure than P_o , and not on the "species" of either. But the most obvious application, and the only one considered here, is to RF power sources, although for our purposes the term "RF source" can be very broadly interpreted to include any dc (or 60- or 400-Hz) powered source of electromagnetic power, P_o , from very low frequency (VLF) to light.

The principal advantage of this device over conventional RF power measurement devices is that it enables "on-line" measurements, i.e., measurements of radiated power, with accuracy hitherto attainable only with dc substitution

calorimeters (Ref. 1). It is, in fact, a kind of dc substitution calorimeter in which the source itself serves as the dc load, but since it does not require an RF load (or an external dc load for dc substitution), it is much cheaper than a conventional RF calorimeter. For this reason one is tempted to call it a "poor man's calorimeter," but we will stick with "no-load calorimeter" (NLC) for the purposes of this article.

The principal limitations on the applicability of the NLC are: (1) source efficiency must be relatively high to obtain good accuracy, (2) it must be possible to operate the source in a $P_0 = 0$, $P_{dc} > 0$ mode to set the P_0 meter zero (this is difficult or impossible for some oscillators, e.g., magnetrons), and (3) the device can only measure the power at the output port of the source, not at some remote point in a transmission line or in free space.

II. Error Model

Figure 2 is an approximate lumped equivalent circuit for heat flow in a typical fluid cooled RF source. Most of P_{diss} , viz P_1 flows from dissipation sites within the source (e.g., a tube anode) through an internal heat exchanger (e.g., coolant passages or fins in the anode) to the coolant. R_{11} represents the thermal resistance of the internal heat exchanger. The coolant then carries P_1 to an external heat exchanger that rejects it to an infinite heat sink at T_0 through equivalent thermal resistance R_{12} . If the cooling system is closed, R_{12} is shunted by thermal capacitance C , which represents the finite heat capacity of the circulating coolant. P_p is the fluid frictional loss in the internal heat exchanger. Heat leakage from the source is represented by the shunt R_2 to the infinite heat sink at T_i .

From Eq. (1) and elementary circuit theory we have

$$P_0 = P_{dc} - (1 + \alpha)P_3 + P_e \quad (2)$$

where

$$\alpha = (R_{11} + R_{12})/R_2$$

and

$$P_e = P_p(1 + R_{11}/R_2) + (T_i - T_0)/R_2, \quad (3)$$

is an error term due to P_p plus the heat flow between sinks at T_i and T_0 through leakage conductance $1/R_2$. In general, T_i and T_0 , hence P_e , are random variables of time.

We assume that only P_3 , the heat carried from the source to the external heat exchanger by the coolant, is sensed, so that the output voltage, v_0 , of the NLC is

$$v_0 = aP_{dc} - bP_3 \quad (4)$$

If, at some time, say $t = 0$, and at some positive value, $P_{dc}(0)$, of P_{dc} , we adjust the zero of the P_0 meter in the manner described above, we set

$$b = a(1 + \alpha)/(1 + \epsilon_0) \quad (5)$$

where $\epsilon_0 = P_e(0)/P_{dc}(0)$, and $P_e(0)$ is the value of P_e at that time. From Eqs. (2), (4), and (5) we find that at any future time, t ,

$$\begin{aligned} \Delta P_0 &= P_0 - v_0/a \\ &\approx \epsilon_0 [P_{dc}(0) - P_{diss}(t)] + \Delta P_e(t) \end{aligned} \quad (6)$$

where $\Delta P_e(t) = P_e(t) - P_e(0)$, and we have assumed ϵ_0 small enough to write $\epsilon_0 \approx \epsilon_0/(1 + \epsilon_0)$. From Eq. (3) we see that P_e , hence $\Delta P_e(t)$, is independent of P_{dc} , hence of P_{diss} , so the two terms of ΔP_0 are uncorrelated, and the *rms* value of ΔP_0 , $rms(\Delta P_0)$, assumes its minimum value,

$$\min [rms(\Delta P_0)] = rms(\Delta P_e(t)) \quad (7)$$

at $P_{diss}(t) = P_{dc}(0)$. To minimize $rms(\Delta P_0)$, therefore, one must not only be able to estimate the value of P_{diss} but one must also rezero the P_0 meter whenever P_{diss} changes. The obvious way to get around this difficulty is to add a signal proportional to $P_e(0)$ to the analog computation of P_0 as, for example, in the circuit shown in Fig. 3. The P_0 meter zero is first set with the P_e compensation pot, R3, at $P_{dc} = 0$. Then, with $P_{dc} > 0$, the P_0 meter is again zeroed with R2 as previously described. This adjustment eliminates the $P_{dc}(0) - P_{diss}$ bias term from Eq. (6).

Theoretically, the P_e compensation enables one to realize $rms(\Delta P_0) = \min [rms(\Delta P_0)] = rms[\Delta P_e(t)]$, i.e., elimination of all errors except those due to random fluctuation of $T_i - T_0$. The cost is slight: one additional adjustment making three in all (R1, R2, and R3), none of which need be repeated when P_{dc} or P_{diss} change. On the other hand, the benefit may also be slight if, for example, $rms[\Delta P_e(t)] \gg \text{ave}(P_e)$, or if instrumentation errors swamp both.

Note that leakage conductance $1/R_2$ enters into the error term P_e only through the relatively small gradient $T_i - T_0$, not through the large gradient between the

source P_{diss} and the leakage sink at T_i . This is another advantage the NLC has over a conventional dummy load calorimeter: in the latter, heat leakage contributes directly to measurement error, and there is no easy or inexpensive way to compensate for it, whereas in the NLC, leakage conductance contributes a small, easily compensatable error, and leakage power itself has no direct effect.

C , the thermal capacity of the circulating coolant, is just one of the many finite heat sinks in a large power source and its cooling system, but it is included in the model because it tends to be much larger than most of the others. It can contribute a maximum error of $(R_{12}/R_2)P_3$ if b is adjusted before C is fully charged. In most large fluid cooled sources, the coolant will be only 5 to 10°C warmer than T_0 , while the internal heat source (e.g., a tube anode) will be hundreds of °C hotter than the coolant. This means that R_{12} is much smaller than R_{11} . Furthermore, $R_{11} + R_{12}$, the total thermal resistance of the cooling system, is always much smaller than the leakage resistance R_2 in any reasonably designed large source. Therefore, $R_{12} \ll R_2$ and the error caused by premature adjustment of b is very small. This reasoning may not hold for small sources that have relatively large heat leakage, but C is proportionally smaller for small sources and the time required to reach thermal steady state is proportionally shorter.

III. Experimental Results

A breadboard NLC was built and used to measure the output of a 10-kW average power water cooled klystron amplifier. The P_{diss} signal was provided by resistance temperature sensors that sensed the ΔT of the combined coolant flows in collector and body. Coolant flow appeared to be constant to within the resolution (about 1%) of the flowmeter (had coolant flow not been constant, a flow rate sensor and (flow rate) $\times \Delta T$ multiplier would be required to provide the P_{diss} signal). The P_{dc} signal was provided by analog multiplication of the voltages appearing at the terminals of beam current and beam voltage meters installed in the klystron power supply.

The P_0 meter was adjusted to 20 kW full-scale using portable standard meters to measure beam current and voltage. No calibration data were available for the kilovoltmeter used to measure beam voltage but its accuracy was assumed to be 1.0% on the basis of the manufacturer's claims. This plus the 0.25% accuracy of the beam current ammeter yields an estimated 1.25% accuracy for the P_{dc} calibration.

Two kinds of tests were used to evaluate the performance of the NLC breadboard. The first was a comparison of simultaneous measurements of RF power by this device and by a conventional dummy load calorimeter. The second was a test of "zero tracking," i.e., the ability of the NLC to retain its original zero reading as P_{dc} is varied over its operational range while the actual RF output remains fixed at zero. The zero-tracking test measures the total error due to nonlinearity and drift. It is, of course, incapable of determining what part of this total is due to instrumentation errors and what part arises in the heat transfer processes of the source itself.

The results of the zero-tracking test appear in Fig. 4. The transient following each P_{dc} step change is greatly exaggerated by integration of the ΔT signal ($\tau \approx 25$ s) required to suppress rapid fluctuations.

Figure 4 shows that the steady-state P_0 error is less than 0.20 kW (= 1.0% of full scale). The P_0 meter was initially zeroed at $P_{dc} = 20$ kW. P_e compensation was not attempted. Were $P_e(0)$ appreciable, we would expect to see the error increasing linearly from 0 to 20 kW, but Fig. 4 shows no clear evidence of such a trend. We conclude that the zero-tracking error is primarily due to temperature drifts ($T_i - T_0$ fluctuations in the simplified error model) within the source and/or instrumentation drift and nonlinearities.

The bulk of the error may well be due to the offset voltage at the input of the ΔT operational amplifier (op-amp). The ΔT op-amp was zeroed at the beginning of the test, but the offset drifted from zero as the ambient temperature changed. We can estimate the temperature change required to produce the observed zero-tracking error as follows.

The resistance temperature bridge output, $v(\Delta T)$, is about 1.0 mV/°C. The coolant flow during the test was 72 l/min (19 gpm). Therefore, at $P_0 = 0$, the constant $v(\Delta T)/P_{dc} = 0.2$ mV/kW. Thus the observed 0.2-kW zero-tracking error corresponds to an offset voltage of 0.04 mV. The op-amp's offset temperature coefficient specification is 15 μ V/°C max, so that the 0.2-kW error could have been caused by an ambient temperature change of only 2.7°C. Obviously, a low-drift op-amp for ΔT would have been preferable, but this breadboard, like most, was built of the most available, not the best, components.

The results of the no-load vs conventional calorimeter measurements are shown in Fig. 5 and Table 1. Although

nothing was known about its thermal properties, the dummy load design appeared to provide excellent thermal insulation between the coolant and the waveguide envelope of the load. The coolant was pure water. Coolant ΔT was measured with a quartz thermometer, and load flow was measured with a differential pressure flowmeter. The values recorded in Table 1 are the means of at least nine nearly simultaneous readings each of P_o and dummy load ΔT at each power level. The dummy load flow appeared to be constant throughout the run.

The apparent negative bias in the $P_o(\text{NLC}) - P_o(\text{CC})$ values in Table 1 may not be significant; all but one difference is less than the maximum 0.20-kW error observed in the zero-tracking test, and the largest, 0.23 kW, is only slightly larger. In other words, the results of

Table 1 are consistent with the hypothesis that the $P_o(\text{NLC}) - P_o(\text{CC})$ discrepancies are entirely due to the previously observed zero-tracking errors.

IV. Conclusions

The no-load calorimeter enables on-line RF power measurements at accuracies otherwise attainable only with much more expensive off-line techniques and equipment. A simple model of heat flow in the RF source shows that the inherent accuracy of the no-load calorimeter measurement is limited essentially by random fluctuation in temperature gradients between heat sinks. Two brief breadboard tests yielded consistent results. ΔT op-amp offset drift appears to be the major error contributor in breadboard tests.

Reference

1. Ginzton, E. L., *Microwave Measurements*, McGraw-Hill, 1957, p. 193.

**Table 1. Comparison of RF output measurements:
NLC breadboard vs conventional calorimeter**

| $P_0(NLC)^a$, kW | $P_0(CC)^b$, kW | $P_0(NOM)^c$, kW | $P_0(NLC) -$ $P_0(CC)$, kW | $\Delta^d, \%$ |
|----------------------|---------------------|----------------------|--------------------------------|----------------|
| 7.88 | 8.05 | 7.6 | -0.17 | -2.1 |
| 7.46 | 7.43 | 7.0 | +0.03 | +0.4 |
| 10.09 | 10.15 | 9.4 | -0.06 | -0.6 |
| 5.15 | 5.38 | 5.0 | -0.23 | -4.5 |
| 3.18 | 3.22 | 3.0 | -0.04 | -1.2 |

^a $P_0(NLC)$ = NLC breadboard measurements.
^b $P_0(CC)$ = conventional (dummy load) measurements.
^c $P_0(NOM)$ = "nominal" RF output per in-line power meter.
^d $\Delta\% = \frac{P_0(NLC) - P_0(CC)}{P_0(NLC)} \times 100\%$.

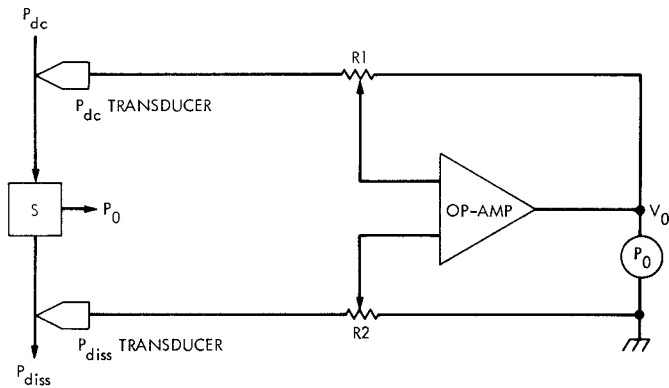


Fig. 1. No-load calorimeter

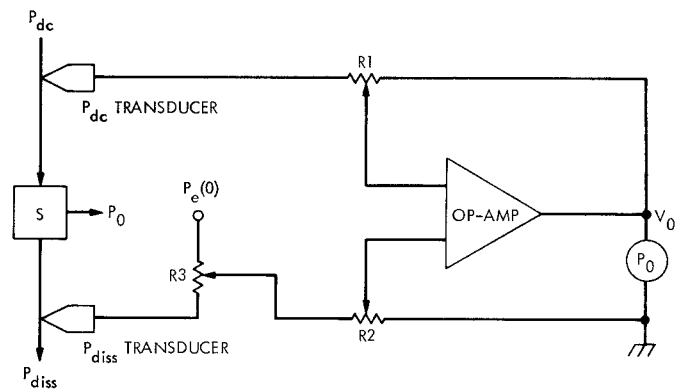


Fig. 3. NLC with P_e compensation

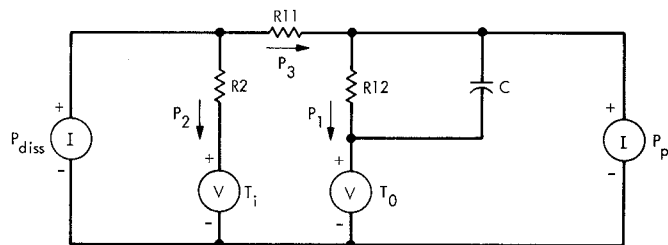


Fig. 2. Electrical analog of heat flow in an RF source

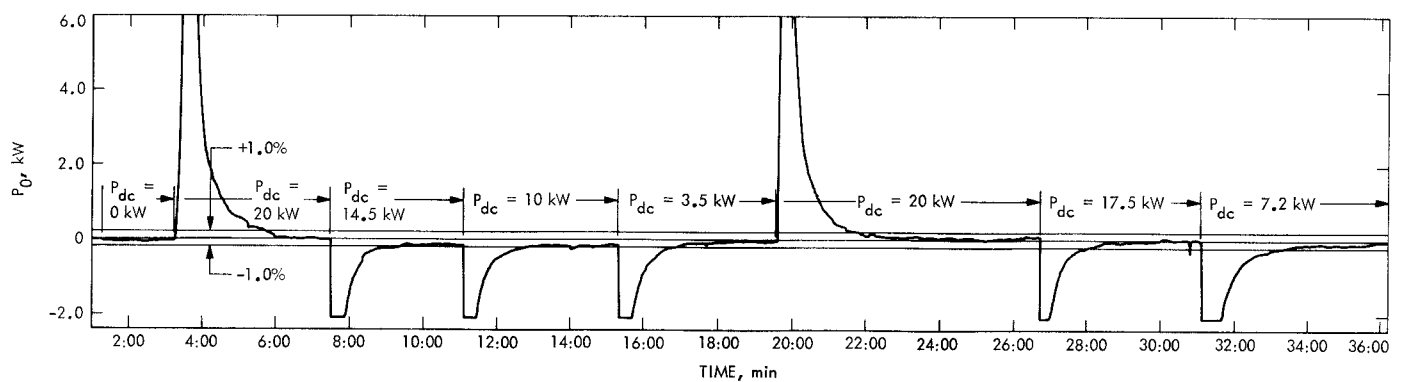


Fig. 4. P_0 zero-tracking performance of the no-load calorimeter

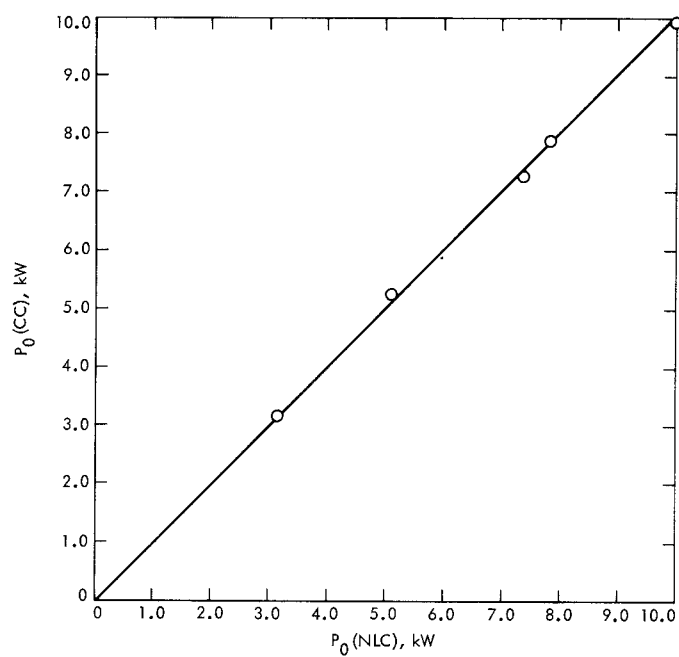


Fig. 5. Comparison of RF output measurements, no-load calorimeter vs conventional calorimeter